
Oct 26th, 12:00 AM

An Experimental Study of the Compressive Performance of Structural Panels with Cold-formed Thin-walled Perforated Steel Channels

B. Salhab

Y. C. Wang

Follow this and additional works at: <https://scholarsmine.mst.edu/isccss>



Part of the [Structural Engineering Commons](#)

Recommended Citation

Salhab, B. and Wang, Y. C., "An Experimental Study of the Compressive Performance of Structural Panels with Cold-formed Thin-walled Perforated Steel Channels" (2006). *International Specialty Conference on Cold-Formed Steel Structures*. 1.

<https://scholarsmine.mst.edu/isccss/17iccfss/17iccfss-session3/1>

This Article - Conference proceedings is brought to you for free and open access by Scholars' Mine. It has been accepted for inclusion in International Specialty Conference on Cold-Formed Steel Structures by an authorized administrator of Scholars' Mine. This work is protected by U. S. Copyright Law. Unauthorized use including reproduction for redistribution requires the permission of the copyright holder. For more information, please contact scholarsmine@mst.edu.

An Experimental Study of the Compressive Performance of Structural Panels with Cold-Formed Thin-Walled Perforated Steel Channels

B. Salhab¹ and Y.C. Wang²

Abstract

This paper presents the results of an experimental investigation of the structural performance of a full-scale panel, constructed of perforated cold-formed thin-walled steel channels, tested under compression and at ambient temperature. The panel was $2m$ ($78.74in$) high and used three $100\times 54\times 15\times 1.2mm$ lipped cold-formed steel channels with perforations along the entire web length. The channel sections were provided by the manufacturer METSEC (2000) from their standard UK product range. FireLine gypsum boards with a thickness of $12.5mm$ ($0.49in$) and manufactured by British Gypsum Limited were attached to both sides of the perforated channels by bolts.

This paper will present some details of this test and also compare the test results against a previous test where the only difference is that the previous test used solid channels. It will also present the results of a numerical study using a general finite element program ABAQUS, in which the behaviour of the test perforated steel channels has been simulated.

The results of comparison with the panel with solid channels indicate that perforation of the entire web length had only minor effect on the panel behaviour and failure load. From the numerical simulation results, it is concluded that ABAQUS can give accurate simulation of the test behaviour provided there is available information on the initial imperfections of the steel channels.

¹ PhD Research Student, Structures and Fire Research Group, Manchester Centre for Civil and Construction Engineering, UMIST & The University of Manchester, Manchester, U.K

² Reader, Structures and Fire Research Group, Manchester Centre for Civil and Construction Engineering, UMIST & The University of Manchester, Manchester, U.K

Keywords

Thermal studs; structural performance; perforated section; cold-formed steel; thin-walled structures; finite element analysis, initial imperfection

1. Introduction

Cold-formed thin-walled steel sections are increasingly used in residential, industrial and commercial buildings in many parts of the world as secondary members of building structures, e.g. as purlins to support the roof and cladding of a building.

However, one disadvantage of this construction when using solid section is the thermal bridging effect which could lead to problems of condensation and high energy loss. A solution to this problem is to have perforations in the web of the solid steel section which can break the heat transfer path, thus reducing the thermal bridging effect. Steel channels with perforations for energy efficiency are called thermal studs.

Whilst perforation will improve energy efficiency of the panel, this also reduces its structural load carrying capacity. In order to obtain optimal solution to satisfy the different demands of a well designed building construction, it is essential that the different aspects of thermal stud performance are thoroughly understood. This paper is a part of the first author's PhD research and will only concentrate on structural performance under compression.

A number of investigators (Yu and Davis 1973, Sivakumaran 1987, Davies et al. 1997, Abdel-Rahman 1998, Pu et al. 1999, and Kesti 2000) have conducted related studies. However, only Kesti's study is of direct relevance to the authors study presented in this paper.

Kesti performed tests on sigma-sections and web-stiffened C-sections with perforated web. He compared the behaviour between panel systems with and without sheathing and found out that sheathing had a significant effect in increasing the ultimate compressive load. Kesti's tests used only one channel and he recommended further tests of full-scale panels using perforated channels. Perforation makes the web behave anisotropically. The axial stiffness of the perforated web in the longitudinal direction is very high compared to the very low axial stiffness in the perpendicular direction. For example, according to Kesti, the axial stiffness of a perforated web is reduced to 0.77 and 0.002 that of a plain solid plate with the same dimensions in the longitudinal and perpendicular direction respectively. Furthermore, the bending stiffness is reduced to 0.77 and 0.06 of that of the solid plate in the longitudinal and perpendicular direction respectively. Because of the low stiffness of the web in

the transverse direction, it is often necessary to rely on the stiffness of the lining materials to provide stability to the thermal studs.

The objectives of this paper are providing some experimental information of perforated steel panels, presenting a preliminary analysis of the test results, and comparing behaviour of perforated and solid steel panels.

2. Preparations of test specimen

The specimens were perforated using a milling machine in the workshop laboratory of the University of Manchester Institute of Science and Technology (UMIST) as shown in figure 1, following the pattern in figure 2. Figure 3 shows one perforated channel. As it can be seen in figure 3 no perforation was made in the two short lengths containing the service holes so as not to further weaken the structural capacity of the channel in these regions.

As will be shown later in numerical simulations of the test results, geometric imperfection is an important factor that influences the behaviour of thin-walled structures. An attempt was made to measure the initial imperfections of the test channels at different locations along the members. Figure 4 shows the measured results for the central channel of the test specimen. These results show a pattern of distortional initial imperfection, the maximum value being between $2\text{-}3\text{mm}$ ($0.079\text{-}0.118\text{in}$) at the different locations. These values are relative to the end sections along the same longitudinal edge of the channel. Since the end sections were distorted and did not have fixed coordinates, it was not possible to evaluate the amount of initial global imperfection that would have been in the test channels. Later numerical simulations will assume nominal values.

Nine tensile coupons, two from the flanges and one from the web of each test channel, were made and tested according to BS EN 10002-1:2001 (BSI 2001). Table 1 gives a summary of the test results. As shown in figure 5, the yield strength is the 0.2% proof strength and the Young's modulus is the slope of the straight line fitted to the initial stress-strain relationship. As can be seen from Table 1, there is little difference in the yield strength and ultimate strength of the 9 test samples. However, since the test stress-strain relationships were non-linear from the beginning, it was difficult to draw a distinct straight line like the one shown in figure 5, the result of which is a relative large variation in the Young's modulus.

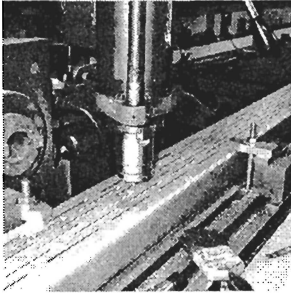


Figure 1:
Milling machine

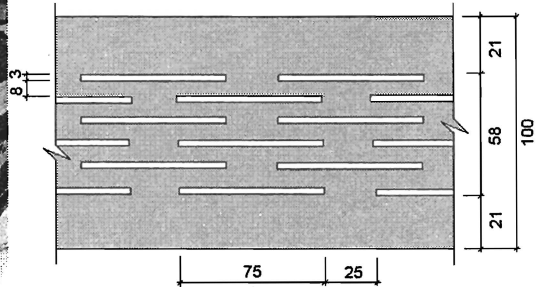


Figure 2: Perforation dimensions (mm)

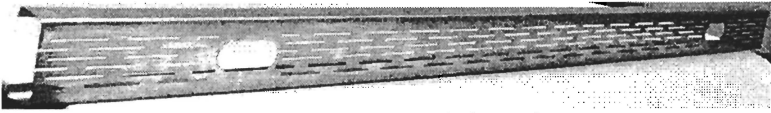


Figure 3: Perforated channel

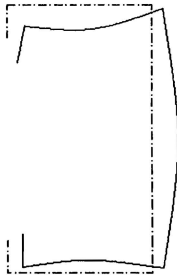


Figure 4a: Pattern of deformation in cross-section

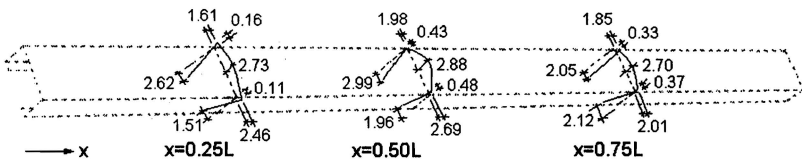


Figure 4b: Measured initial imperfections along length (mm)

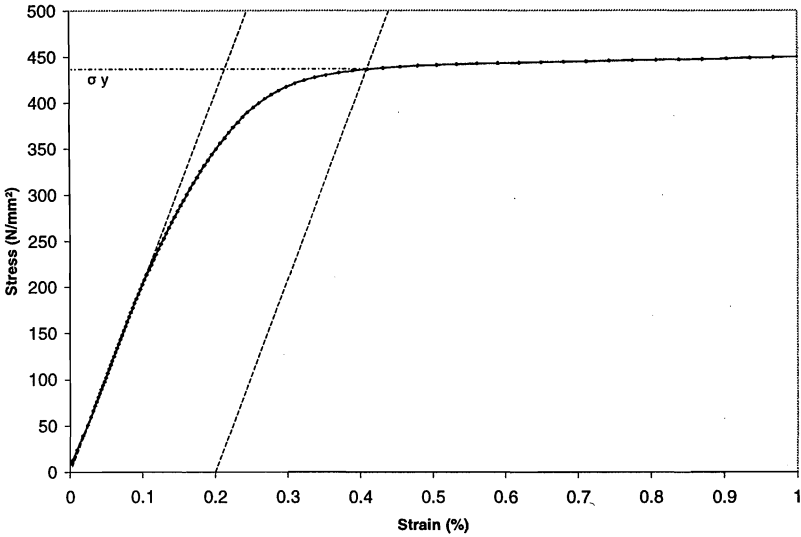


Figure 5: Determination of yield stress and Young's modulus of steel

	0.2% proof stress σ_y N/mm ² (ksi)	Ultimate tensile stress σ_u N/mm ² (ksi)	Young's Modulus E KN/mm ² (ksi)
Average	437.7 (63.5)	531.2 (77)	205.3 (29782.9)
Standard deviation	4.8 (0.7)	3.1 (0.45)	31.1 (4517.2)

Table 1: Summary of mechanical properties of steel
(Numbers between brackets are in ksi)

3. Panel test and results

Figure 6 shows the test panel and the loading and reaction frame. The applied loads were transmitted from the three hydraulic loading jacks, aligned along the three perforated channels, to the test panel via a moving steel beam on top of the test panel. The applied loads were monitored by load cells attached to the hydraulic jacks. Figure 7 shows a sketch of the test setup and locations of the displacement transducers.

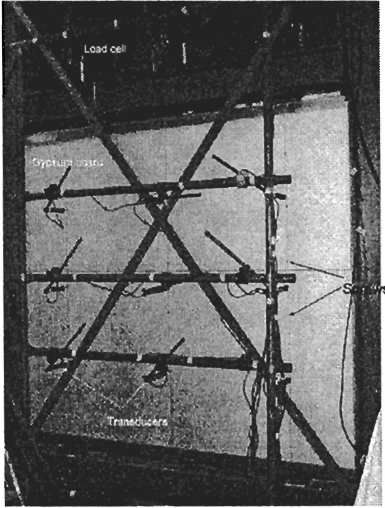


Figure 6: Test panel

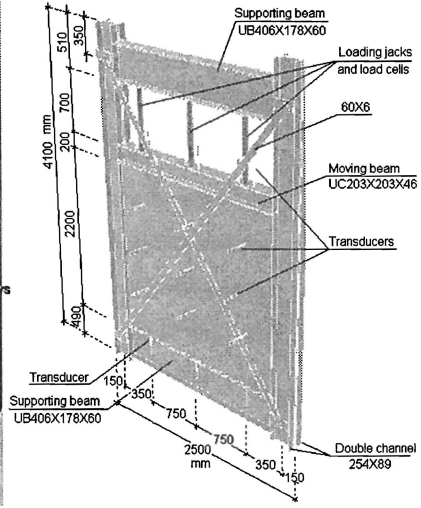


Figure 7: Transducers

The applied loads were increased in increments of 2KN (0.45 kips) during the initial stage then in increments of 1KN (0.225 kips) until they reached 54 KN (12.14 kips) when the left channel could not take any load due to the inability to pump in the hydraulic jack. That was accompanied by the channel pushing the gypsum board out of its position as shown in figure 8 where the lateral displacement is noticeable, i.e. the gypsum board moving out of the loading frame.

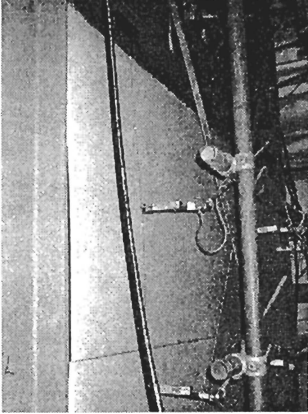


Figure 8: Gypsum board behaviour

The middle and right channels failed by global flexural buckling about the major axis near the mid-height. Even though the webs of the test channels were perforated, there was no evidence of local buckling of the web.

Figure 10 shows the axial displacement-load curves of the three channels, indicating that they behaved in an almost identical trend.

On the other hand, figure 11, which presents the panel lateral deformations at various locations, indicates that because there was no primary bending in the channels, the lateral displacements were sensitive to the initial imperfections in the channels.

Figure 9, which shows the three test channels after the test, indicates that the left channel failed by distortional buckling just below the service hole.

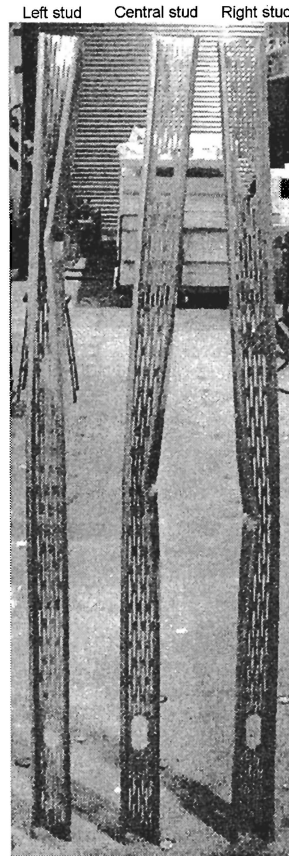


Figure 9: Channel failure mode

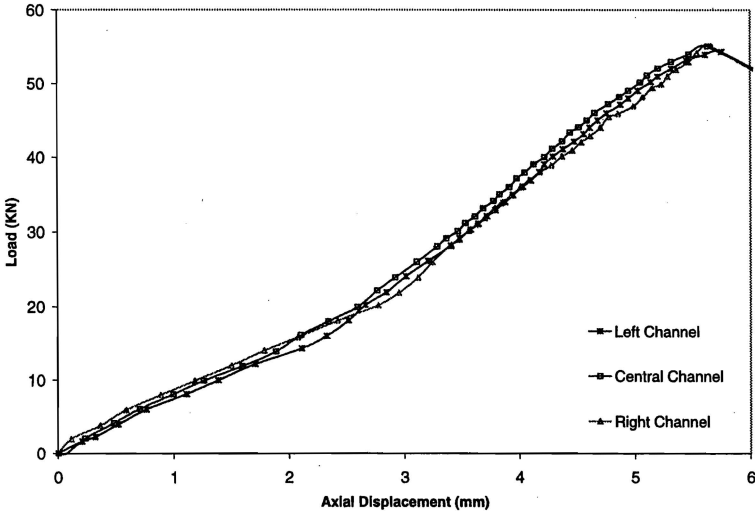


Figure 10: Load-axial displacement relationships

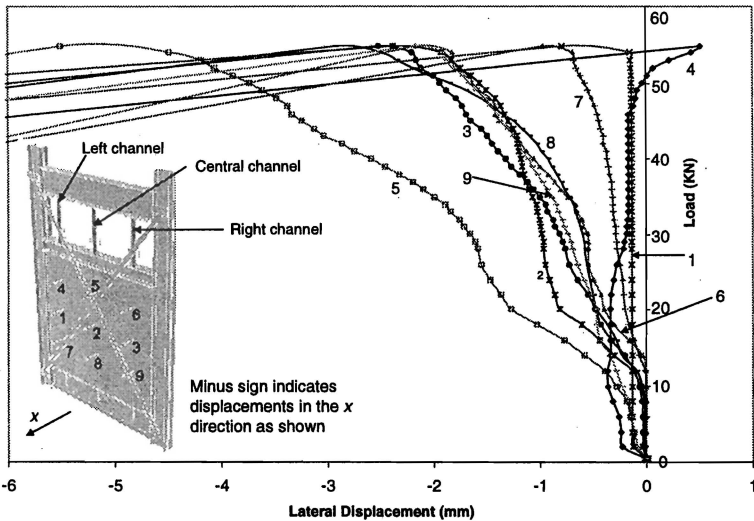


Figure 11: Load-lateral displacement relationships

The left channel, whose lateral deflections were measured by transducers 1, 4 and 7, had very small global deflections until failure. The other two channels developed relatively large global deflections from the beginning. This is in

agreement with the observed failure modes of the channels shown in figure 9. The left channel would have had relatively small global initial imperfections and thus distortional buckling governed failure. On the other hand, the global initial imperfections in the other two channels would have been more substantial, inducing the observed global flexural buckling failure mode.

4. Comparison with a previous test using solid channels

Feng (2004) had earlier performed the same test, but using solid channel sections. Figure 12 compares the recorded axial displacements from the current test using perforated channels and the test of Feng. It can be seen that there is little difference between the two tests. Feng reported that the solid sections failed near the service hole by global buckling about the major axis. For the perforated channels, the failure position moved to around the mid-height as shown in figure 9.

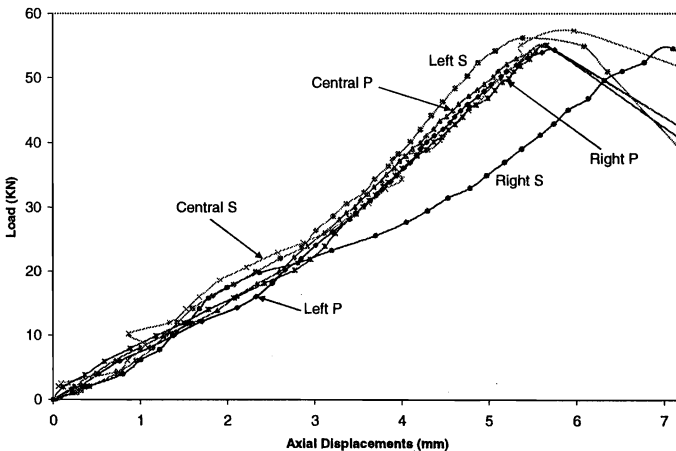
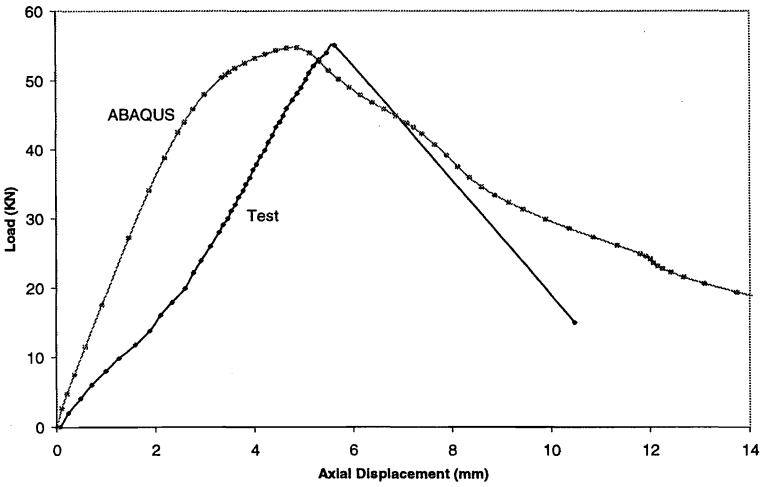


Figure 12: Comparison between load-axial displacement curves (P=perforated channel, S=solid channel)

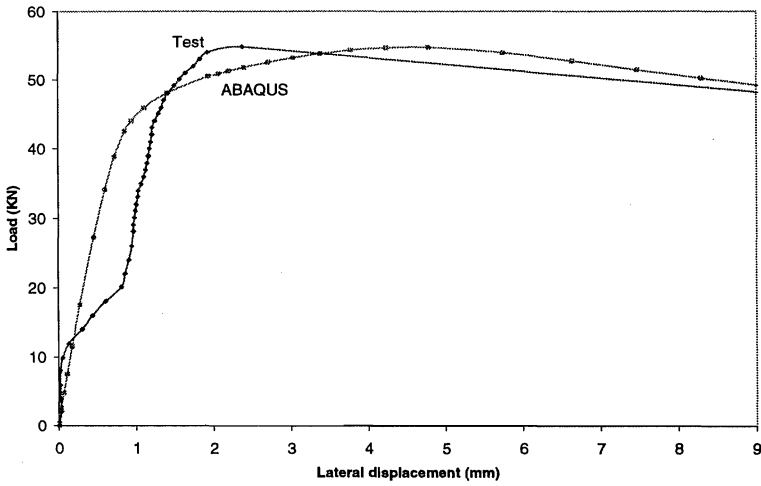
5. Numerical simulation results

Behaviour of the test channels was simulated using a general purpose finite element package ABAQUS (HKS 2002). Figures 13-15 present the results of two simulations, the difference between the two being the amount of initial imperfections incorporated in the analysis. Figure 13 is for a combination of a maximum global imperfection of 2mm and a maximum distortional imperfection

of 2mm . Figure 14 is for a combination of a maximum global imperfection of 0.5mm and a maximum distortional imperfection of 2mm . Local buckling was not observed and therefore no initial local imperfection was considered in the simulation studies. The different combinations of global and distortional initial imperfections were incorporated to ensure that either mode of failure could be induced. As mentioned earlier, the left channel developed small global lateral deflections (figure 11). Therefore, figure 14, in which the maximum initial global imperfection was 0.5mm ($L/4000$), may be considered as appropriate simulation results for the left channel. On the other hand, the central and the right channels developed large global lateral deflections (figure 11). Thus, figure 13, in which the maximum initial global imperfection was 2mm ($L/1000$), may be considered as suitable simulation results for these two channels. To confirm this, figure 15 compares the observed and simulation failure modes of the channels. It can be seen that the predominate failure mode from the simulation agrees with the observed failure mode in each case. There is some discrepancy between the experimental and simulated failure shape of the channels, i.e. the observed distortional buckling in the left channel was near the top service hole but was calculated to be at mid-height, and distortional buckling was simulated for the central channel near the top service hole, but not observed. This discrepancy may be attributed to the difficulty of incorporating accurate description of detailed initial imperfections in numerical analysis. The more important point of this comparison between experimental and simulation results is that the simulations reproduced very well the observed behaviour of the channels, in terms of the load-deflection curves and failure loads in figures 13 and 14. The initial rapid increase in recorded deformations is clearly a result of the test panel taking up gaps that would have inevitably been in the test system.

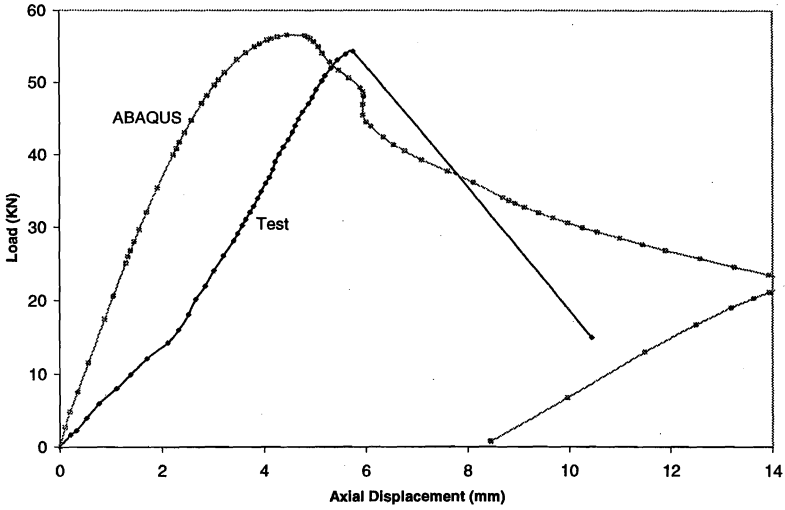


(a) Load-axial deformation relationship

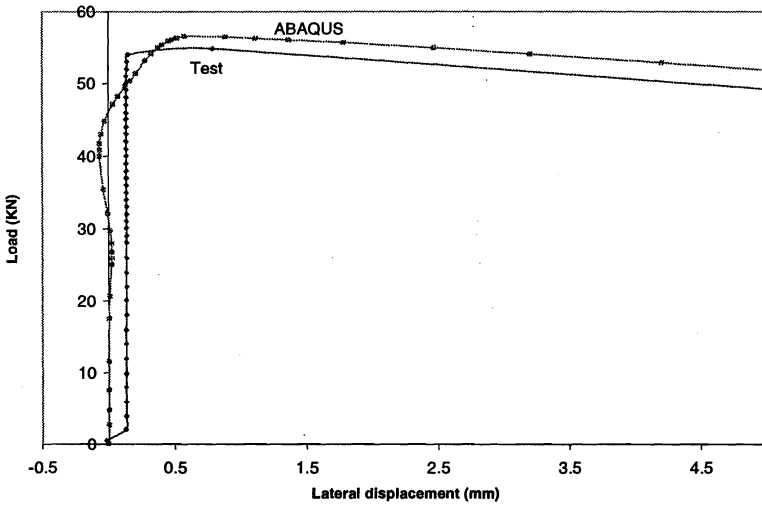


(a) Load-lateral deformation relationship

Figure 13: Comparison between test results (central channel) with ABAQUS simulation with 2mm distortional and 2mm global initial imperfections

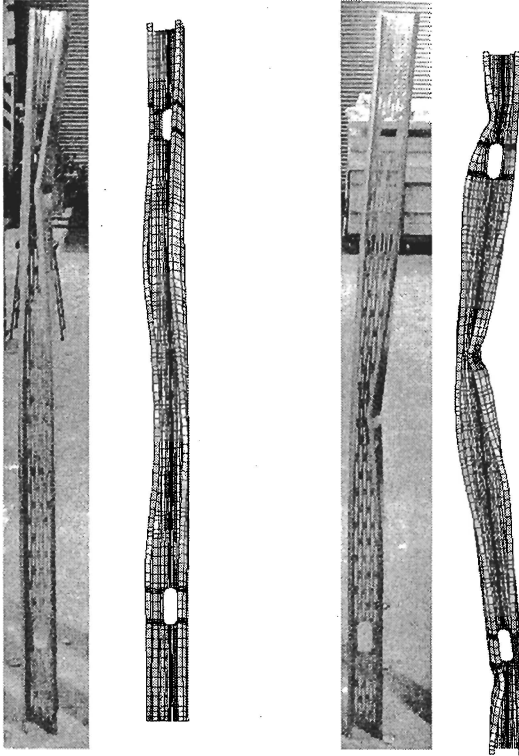


(a) Load-axial deformation relationship



(b) Load-lateral deformation relationship

Figure 14: Comparison between test results (left channel) with ABAQUS simulation with 2mm distortional and 0.5mm global initial imperfections



(a) left channel

(b) central channel

Figure 15: Test and simulated failure modes

6. Conclusions

This paper has presented some details of a full-scale structural panel test in which the steel channels were perforated along the webs. The test results were compared to those of a test in which the channels were solid and to simulation results. The following conclusions may be drawn:

- Although the three test channels were nominally identical, distortional buckling was observed in one channel and global flexural buckling about the major axis in two other channels.
- The difference in the failure modes is caused by the difference in detailed initial imperfections of these nominally identical channels.
- Using different initial imperfection values, it was possible to simulate, using a general finite element package ABAQUS, the different observed failure modes of the test channels.
- The simulated load-deflection curves and failure loads were very close to the recorded ones from the test.
- A comparison with a previous test in which solid channels were used did not indicate substantial difference in behaviour between perforated channels of this study and solid channels of the previous test.

Acknowledgements

The authors would like to thank Mr. J. Gorst and Mr. J. Gee for their help in performing the test. This research forms part of the first author's PhD project sponsored by *the Syrian Damascus University*.

References

1. Abdel-Rahman, N. and Sivakumaran, K. S. (1998), "Effective design width for perforated cold-formed steel compression members", *Canadian Journal of Civil Engineering*, vol. 25, pp. 319-330
2. AISI (1991), "The specification for design of cold-formed steel structural members", *American Iron and Steel Institute, Washington, DC*.
3. British Standard EN 10002-1 (2001), "Metallic materials- Tensile testing, Part1: Method of test at ambient temperature", *British Standard Institution, London, UK*.
4. Davies, J. M., Leach, P. and Taylor, A. (1997), "The design of perforated cold-formed steel sections subjected to axial load and bending", *Thin-Walled Structures*, Vol. 29, pp. 141-157

5. Feng, M., (2004), "Numerical and experimental studies of cold-formed thin-walled steel studs in fire", *PhD Thesis, The University of Manchester, UK.*
6. HKS (2002), "ABAQUS Standard User's Manual", *volumes I-II-III Version 6.3, Hibbit, Karlsson & Sorenson Inc.*
7. Kesti, J. (2000), "Local and distortional buckling of perforated steel wall studs", *PhD Thesis, Helsinki University of Technology, Finland.*
8. METSEC (2000), "Design and specification guide for steel framing systems", *Metsec Plc, UK.*
9. Pu, Y., Godley, M. H. R., Beale, R. G., and Lau, H. H. (1999), "Prediction of ultimate capacity of perforated lipped channels", *Journal of structural Engineering, vol. 125, No. 5, pp. 510-514*
10. Sivakumaran, K. S. (1987), "Load capacity of uniformly compressed cold-formed steel section with punched web", *Canadian Journal of Civil Engineering, vol. 14, pp. 550-558*
11. Trahair, N. S. (1993), "Flexural-torsional buckling of structures", *The University of Sydney, Australia.*
12. Yu. Wei-Wen, Davis, C. S. (1973), "Cold-formed steel members with perforated elements", *Journal of the structural division, vol. 99, pp. 2061-2077*

